KSCE Journal of Civil Engineering (2018) 22(3):1002-1015
Copyright ⓒ2018 Korean Society of Civil Engineers
DOI 10.1007/s12205-018-0013-y

Probabilistic Learning for Decision-making on Civil Infrastructures

pISSN 1226-7988, eISSN 1976-3808
www.springer.com/12205

Response Spectrum Code-Conforming PEER PBEE using Stochastic Dynamic Analysis and Information Theory

Umberto Alibrandi* and Khalid M. Mosalam**

Received November 8, 2017/Revised Jaunary 17, 2018/Accepted Jaunary 17, 2018/Published Online

Abstract

In this paper, the tools of the stochastic dynamic analysis are adopted for Performance-Based Earthquake Engineering (PBEE). The seismic excitation is defined through a evolutionary Power Spectral Density compatible with the response spectrum given by mandatory codes. In this way, the performance-based design is applied considering the excitation coherent with the codes. Inside the framework, the seismic fragility curves are determined through the Kernel Density Maximum Entropy Method (KDMEM), recently proposed by the authors. It is a novel statistical method capable to reconstruct the seismic fragility curves, including the tails, from a small number of code-conforming artificial ground motions. Moreover, KDMEM is based on the Maximum Entropy (ME) principle and it provides the least biased probability distribution given the available information. Comparison between stationary and nonstationary artificial accelerograms is analyzed, and the corresponding model uncertainty discussed. KDMEM provides also credible bounds of the uncertain performances, which is beneficial for risk-informed decisions. The proposed formulation does not require the selection of a suitable set of ground motions. Accordingly, it can be adopted for optimal design in current engineering practice. Therefore, it fills the gap between the classical code-conforming designs and the enhanced performance-based designs.

Keywords: *eurocode conforming design, information theory, kernel density maximum entropy, opensees, performance based earthquake engineering, reinforced concrete office building, seismic risk analysis, stochastic dynamic analysis*

1. Introduction

The response spectrum is the most used tool by practicing engineers for basic representations of the seismic action. The ordinary structures are designed to behave inelastically for the seismic intensity prescribed by the design codes. This is obtained in the framework of the response-spectrum analysis through the adoption of the behavior (reduction) factor, q, in the Eurocode 8 (Eurocode, 2004), as an example. However, a realistic evaluation of the structural response should be dynamic and related to the damage that occurs under repeated and usually inelastic loading cycles. This is attributed to the philosophy of earthquake-resistant design not to prevent the occurrence of the damage, but to limit its occurrence under the design earthquake (Ellingwood, 2001). Starting from these considerations, damage-based limit states along with sophisticated inelastic structural models are needed.

It is largely recognized that the natural hazards and the strength of materials are subjected to several sources of uncertainty. Therefore, a probabilistic analysis is essential in predicting the most likely behavior of buildings. This can be accomplished by using the general probabilistic framework of Performance-Based Earthquake Engineering (PBEE), originally proposed by Cornell and Krawinkler (Cornell and Krawinkler, 2000) with the following main steps: (*i*) characterization and assessment of the seismic hazard, (*ii*) probabilistic assessment of the seismic demand on the structure, (*iii*) probabilistic assessment of the resulting physical damage, (*iv*) assessment of expected economic and other losses resulting from damage (Yang *et al*., 2006; Günay and Mosalam, 2013). In this way, the problem is disaggregated into four models: (*i*) the seismic model that predicts the Intensity Measure, *IM*, (*ii*) the structural model that predicts the structural response defined through the Engineering Demand Parameter, *EDP*, (*iii*) the damage model that predicts the Damage Measure, *DM*, and (*iv*) the loss model that predicts the Decision Variable, *DV*. The latter step is one of the key features of the PBEE methodology, which allows the explicit calculation of the performance measures, expressed in terms of the direct interests of various stakeholders.

The PBEE methodology has several attractive features with respect to standard seismic codes. Therefore, it is becoming popular for optimal design of facilities even amongst practicing engineers (FEMA ATC-58-1, 2011). It is expected that in the near future, PBEE will be adopted in the seismic codes worldwide. The goal of this paper is to present a code-conforming formulation

*Senior Research Fellow, Berkeley Education Alliance for Research in Singapore, Create Tower, 1 Create way, #11-02, 138602 Singapore (Corresponding Author, E-mail: umbertoalibrandi@gmail.com)
**Professor, University of California at Berkeley, Dept. of Civil and Environmental Engineering, 723 Davis Hall, Berkeley 94720, CA (E-mail: mosalam@berkeley.edu)

for PBEE to allow practicing engineers to develop enhanced performance-based designs of facilities subjected to seismic excitation conforming to the recommendations of current seismic codes.

In the current PBEE practice, the seismic hazard is characterized in terms of one or more *IM*s, for which annual probabilities of exceedance are developed. In the seismic codes, the seismic hazard is defined by suitable response spectra, whose parameters take into account the site conditions, while the *IM* is given in terms of the Peak Ground Acceleration (PGA), A_g, defined for each site and for different return periods. When the behavior of the system is highly nonlinear, the technique of the response spectrum cannot be applied. In these cases, the codes allow to model the seismic action through ground-acceleration time-history analyses under excitations which are required to match the elastic response spectra for a viscous damping ratio $\zeta_0 = 5\%$. This approach has some controversial issues. First, the codes typically require the adoption of a reduced number of sets of accelerograms, which generally do not allow to develop a reliable statistical analysis. Second, the codes require that the accelerograms to be scaled to match the elastic response spectrum, where this scaling remains as a debatable step. Conversely, in this paper the stochastic input is defined as a Power Spectral Density (PSD) compatible with the response spectrum given by the codes (Cacciola *et al*., 2004; Cacciola *et al*., 2014, Basone *et al*., 2017). In this way, at least for a Single Degree of Freedom (SDOF) linear system, results in terms of the peak response by stochastic analysis and by the response spectrum are almost identical. Starting from the definition of a stochastic ground motion model coherent with a given response spectrum, subsequent models of the classical PBEE approach are developed.

The structural model in PBEE is considered through the conditional probability distribution of the EDP on the structure (e.g. interstory drift, roof or floor accelerations) for each *IM* level corresponding to a specified annual rate of exceedance. This is usually performed by nonlinear time-history analyses with a selected suite of recorded ground motions which are individually scaled to the specified *IM* level (Vamvatsikos and Allin Cornell, 2002). The computed sample of the maximum responses is subsequently used to estimate the median and logarithmic standard deviation of the seismic demand, to which a lognormal (LN) distribution is fitted. Denoting *edp* as a chosen threshold of the *EDP* for the given $IM \equiv im$ in terms of $PGA \equiv a_g$, the result of the analysis is the conditional Probability Of Exceedance (POE), $P(edp|im)$, also known in literature as the *fragility curve*.

In this paper, the code-conforming seismic reliability analysis is developed through a full stochastic approach, giving the conditional POE $P(edp|a_g)$. Stochastic dynamic analysis for a general nonlinear Multi-Degree of Freedom (MDOF) system is challenging. Some methods of simulations have been developed to reduce the computational effort (Rackwitz, 2001; Au and Beck, 2001; Bucher, 2009; Kurtz and Song, 2013; de Angelis *et al.*, 2015; Alibrandi *et al*., 2016). However, in many cases, these methods require hundreds or even thousands of analyses for each threshold. An alternative strategy is represented from the methods of equivalent linearization (Roberts and Spanos, 1990; Fujimura and Der Kiureghian, 2007; Wang and Song, 2017; Alibrandi and Mosalam, 2017b). In this paper, the stochastic analysis is developed through the Kernel Density Maximum Entropy Method (KDMEM) (Alibrandi and Ricciardi, 2008; Alibrandi and Mosalam, 2017c). This is a statistical approach providing a good reconstruction of the target Probability Density Function (PDF), including its tails, from samples of small size. KDMEM is a data-driven approach, so that when the number of samples increases, it converges asymptotically to the target distribution. Moreover, it implements the principle of Maximum Entropy (Jaynes, 1957; Jaynes, 1968; Kapur and Kesavan, 1992) so that it provides the least biased distribution given the available information. It presents some attractive features with respect to many existing methods of structural reliability and stochastic dynamic analysis, since its performances are not affected by the number of random variables, degree of nonlinearity of the dynamic system, and/or shape of the limit state function. Moreover, it does not require any coupling with the structural analysis software. Thus, the results of any existing commercial software can be adopted. In this paper KDMEM is used jointly with the bootstrap technique (Efron, 1982), making it possible to determine credible bounds of the fragility curves when a reduced number of artificial ground motions are considered, e.g. $n_s = 20–100$.

The third step in PBEE converts the *EDP* to the *DM*, addressed by fragility functions for different building components, while the final stage is the conversion from the DM to the DV through tabulated information of the repair cost for each performance group and damage statee. These steps follow the classical framework of PEER PBEE. After describing the main features of the proposed procedure, it is applied to a hypothetical reinforced concrete office building located in Italy.

2. Code-Conforming Performance Based Earthquake Engineering

2.1 Code-Conforming Stochastic Seismic Hazard Analysis

The Pacific Earthquake Engineering Research (PEER) center has developed a robust PBEE methodology, based on the probabilistic evaluation of performance measures expressing the direct interests of the involved stakeholders. In PEER PBEE, the first step is the characterization of the seismic hazard. To guarantee full consistency with the mandatory design codes, here the seismic hazard is defined by suitable response spectra, provided by the codes. The *IM* of the seismic event is given by the *PGA*, A_g, defined for each site and for different return periods T_R. In this case, the value $IM \equiv A_g$ and its POE $P(A_g) = Prob[A_g \geq a_g]$ are defined by the codes. Assuming that the temporal occurrence of an earthquake is described by a Poisson model (Kramer, 1996):

$$P(a_{g,m}) = P[A_g(t) \geq a_{g,m}] = 1 - \exp\left(-\frac{t}{T_R}\right) \quad (1)$$

where t is typically selected as the duration T_L of the lifecycle of the facility, while T_R is the return period of the seismic event. The probability of occurrence of the m-th threshold of A_g is given by its POE as follows:

$$p(a_{g,m}) = Prob[a_{g,m-1} \le A_g \le a_{g,m}] = P(a_{g,m-1}) - P(a_{g,m}) \quad (2)$$

Let $a_{g,1}$ and $a_{g,2}$ be the suggested values by the codes for A_g whose return periods are $T_{R,1} = 95$ years and $T_{R,2} = 475$ years, the application of Eq. (1) for $t \equiv T_L \equiv 50$ years gives $P(a_{g,1}) = 41\%$ and $P(a_{g,2}) = 10\%$. Through Eq. (2), it is seen that $p(a_{g,1}) = Prob[A_g \le a_{g,1}] = 1 - 0.41 = 0.59$, $p(a_{g,2}) = Prob[a_{g,1} \le A_g \le a_{g,2}] = 0.41 - 0.1$, while of course Prob$[A_g \ge a_{g,2}] = 1 - [p(a_{g,1}) + p(a_{g,2})] = 0.10$.

The hazard analysis also includes the selection of a set of ground motions coherent with the hazard curve. The seismic codes provide the spectral pseudo acceleration $RSA(T, \zeta_0)$, where T is the natural period of the dynamic oscillator and ζ_0 is its damping ratio. The codes allow time-history representations of the seismic action for analyzing the nonlinear behavior of the structures whereas the response spectrum technique might not provide accurate results (e.g. case of structures with base isolation or energy dissipation systems). The codes do not suggest a method for generating the artificial accelerograms, but only recommend that they match the elastic response spectra for 5% viscous damping ratio. Typically, to obtain artificial accelerograms, the ground motion acceleration $A_g(t)$ at a given location is modeled as a stochastic process, and any ground motion can be seen as a sample of the stochastic process itself. In literature, many stochastic models have been proposed in the last decades. Most common approaches adopt Gaussian models (Shinozuka and Deodatis, 1988), which are defined probabilistically through their evolutionary Power Spectral Density (PSD) (Priestley, 1965) as follows:

$$\begin{cases} G_{A_g}(t,\omega) = |\varphi(t,\omega)|^2 G_{A_g}(\omega) & \omega \ge 0 \\ G_{A_g}(t,\omega) = 0 & \omega < 0 \end{cases} \quad (3)$$

where $\varphi(t,\omega)$ is the frequency-dependent modulating function, while $G_{A_g}(\omega)$ is the one-sided PSD of the stationary part of $A_g(t)$. Once the evolutive PSD $G_{A_g}(t,\omega) = |\varphi(t)|^2 G_{A_g}(\omega)$ of the ground acceleration is evaluated, the stochastic ground motion model $A_g(t, \boldsymbol{u})$ can be defined through the following discrete Fourier series (Rice, 1954; Shinozuka and Deodatis, 1991; Grigoriu, 1993; Alibrandi, 2014):

$$\begin{aligned} A_g(t,\boldsymbol{u}) &= \sum_{k=1}^{n} \sqrt{G_{A_g}(t,\omega_k)\Delta\omega}\,[cos(\omega_k t)u_k^c + sin(\omega_k t)u_k^s] \\ &= \sum_{k=1}^{n} s_k^c(t)u_k^c + s_k^s(t)u_k^s = \boldsymbol{s}(t,\omega)\cdot\boldsymbol{u} \end{aligned} \quad (4)$$

where n is the number of harmonic components, $\sigma_k(t) = \sqrt{G_{A_g}(t,\omega_k)\Delta\omega}$, $k = 1, 2, ..., n$, $\Delta\omega \le 2\pi/t_{fin}$, being t_{fin} the time observing window, $\boldsymbol{u} = \{\boldsymbol{u}^c, \boldsymbol{u}^s\}$ is a vector of order $2n$ of normal standard random variables, $\boldsymbol{u}^c = \{u_1^c, u_2^c, \ldots, u_n^c\}$, $\boldsymbol{u}^s = \{u_1^s, u_2^s, \ldots, u_n^s\}$, $\boldsymbol{s}(t,\omega) = \{\boldsymbol{s}^c(t,\omega), \boldsymbol{s}^s(t,\omega)\}$, is a vector that collects the corresponding shape functions $s_k^c(t) = \sigma_k(t)\cos(\omega_k t)$ and $s_k^s(t) = \sigma_k(t)sin(\omega_k t)$ determined by the correlation structure of the input given by the underlying evolutionary PSD. Eq. (4) can be used to generate samples of the stochastic ground motion model where each realization is obtained through the generation of the normal standard random variables $\boldsymbol{u}$.

2.1.1 Stationary Models

It is known that earthquake ground motions have nonstationary characteristics both in the time and the frequency domain, where the temporal nonstationarity models the variation of the intensity of the ground motion in time, while the spectral nonstationarity represents the nonstationarity in the frequency domain and it refers to the variation of the frequency content in time. A good modelling of earthquakes is typically accomplished through fully non-stationary Gaussian stochastic processes. However, the use of stationary accelerograms remains widely employed. In such cases, the knowledge of the stationary PSD $G_{A_g}(\omega)$ only is required, while the modulating function appearing in Eq. (3) is $\varphi(t,\omega) = 1$. To determine the one-sided stationary PSD of the ground acceleration, the tools of the stochastic dynamic analysis are used to relate the pseudo-acceleration Response Spectrum $RSA(\omega, \zeta_0)$ to the median value of the peak response of a SDOF system (Vanmarcke and Gasparini, 1977; Der Kiureghian, 1981; Der Kiureghian and Neuenhofer, 1992). In this paper, the model proposed in (Cacciola *et al*., 2004; Cacciola *et al*., 2014) is adopted. The stationary PSD $G_{A_g}(\omega)$ is determined through the following recursive expression:

$$\begin{cases} G_{A_g}(\omega_i) = 0 & 0 \le \omega_i \le \omega_s \\ G_{A_g}(\omega_i) = \dfrac{4\zeta_0}{\pi\omega_i - 4\zeta_0\omega_{i-1}} \times \left[\dfrac{RSA(\omega_i,\zeta_0)^2}{\eta_X^2(\omega_i,\zeta_0)} - \Delta\omega \sum_{k=1}^{i-1} G_{A_g}(\omega_k) \right] & \omega_i > \omega_s \end{cases} \quad (5)$$

where RSA(ω_i, ζ_0) is obtained from response spectrum given by the codes, for given damping ratio ζ_0, circular frequency $\omega_i = 2\pi/T_i$, and period, T_i, while $\eta_X(\omega_i, \zeta_0)$ is the peak factor under the assumption of a barrier out-crossing in clumps, i.e.

$$\eta_X(\omega_i,\zeta_0) = \sqrt{2log\{2N_X[1 - exp(-\delta_X^{1.2}\sqrt{\pi log(2N_X)})]\}} \quad (6)$$

with

$$\begin{cases} N_X = \dfrac{t_s}{2\pi}\omega_i(-log(0.5))^{-1} \\ \delta_X = \sqrt{1 - \dfrac{1}{\zeta_0^2}\left(1 - \dfrac{2}{\pi}arctan\dfrac{\zeta_0}{\sqrt{1-\zeta_0^2}}\right)^2} \end{cases} \quad (7)$$

In Eq. (7), it has been assumed that the input PSD is smooth and $\zeta_0 \ll 1$. Moreover, t_s is assumed equal to the stationary part of the accelerogram, while ω_s is the lowest bound of the existence domain of η_X.

2.1.2 Quasi Stationary and Fully Non-stationary Models

The quasi-stationary models describe the temporal non-stationarity through a modulating function dependent only upon the time t, i.e. $\varphi(t,\omega)\equiv\varphi(t)$, see Eq. (3). In this way the evolutionary PSD $G_{A_g}(t,\omega)=|\varphi(t)|^2 G_{A_g}(\omega)$ is obtained through a time-dependent scaling of the stationary random process $G_{A_g}(\omega)$. These models are known in literature also as separable or uniformly modulated.

The simulation of fully non stationary accelerograms can be obtained through the adoption of time-frequency modulating functions. In such case the evolutionary PSD is given by $G_{A_g}(t,\omega)=|\varphi(t,w)|^2 G_{A_g}(\omega)$, where the stationary power spectrum $G_{A_g}(\omega)$ is determined by equating for each frequency the energy of a separable spectrum compatible model and that of a non-separable process (Preumont, 1985; Cacciola and Zentner, 2012)

$$G_{A_g}(\omega)\int_0^\infty |\varphi(t,\omega)|^2 dt = G^S_{A_g}(\omega)\int_0^\infty |\varphi(t)|^2 dt \tag{8}$$

In Eq.(8) $G^S_{A_g}(\omega)$ is the stationary PSD compatible with the response spectrum, like Eq. (5), while $\varphi(t)$ is a time dependent modulating function.

In the literature it is recognized that the accelerograms generated through a stochastic approach do not present the variability of the recorded accelerograms. To this aim, the parameters of the modulating function can be defined through uncertain parameters depending on the seismological parameters. For the all the analyzed non-stationary models discussed in this section, if the spectrum compatibility is not verified, an iterative correction term can be adopted (Cacciola, 2010)

$$\begin{cases} G^{(1)}_{A_g}(\omega) = G_{A_g}(\omega) \\ G^{(k)}_{A_g}(\omega) = G^{(k-1)}_{A_g}(\omega)\left[\dfrac{RSA(\omega,\zeta_0)^2}{RSA^{(k-1)}(\omega,\zeta_0)^2}\right] \end{cases} \tag{9}$$

where $RSA^{(k)}(\omega,\zeta_0)$ is the approximate average pseudo-acceleration spectrum determined at the k-th iteration.

2.1.3 Model Uncertainty

All the sets of artificial accelerograms above discussed are equivalent from the point of view of the codes, since all of them match the elastic response spectrum. However, the amplitude and frequency content of an accelerograms can affect the response of the structural system. Thus, it is expected that accelerograms generated by different PSD (model and parameters) can determine a significant variability of the seismic fragility curves. Typically, it is expected that stationary accelerograms provide conservative responses, and that non-stationarity of ground motions is more relevant for nonlinearly behaving structures. However, this is not always the case, see for example (Cacciola *et al.*, 2014). Therefore, the selection of the PSD fitting process requires including the model uncertainty inside the decision making process. As will be discussed below and shown through the numerical application, this issue can be well managed by the proposed framework.

2.2 Structural Analysis using Kernel Density Maximum Entropy Method

The second step of PEER PBEE is the probabilistic assessment of the demand on the structure. For each PGA level, $A_g = a_{g,m}$, a set of n_s artificial accelerograms is considered. The corresponding dynamic computations provide the conditional POE of selected *EDP*s, i.e. the fragility curves. The *EDP* may be local parameters as element forces or deformations, or global parameters as interstory drift or floor acceleration. Typically, local parameters are more suitable for structural components, the floor accelerations are better suited for non-structural components, e.g. laboratory equipment, and interstory drifts may be used for structural and non-structural components. Peak values of the above quantities are considered as *EDP*s. In the code-conforming PEER PBEE framework, one has the following:

$$p(edp_i) = Prob[EDP \geq edp_i] = \sum_m P(edp_i|a_{g,m})p(a_{g,m}) \tag{10}$$

where $p(a_{g,m})$ is the probability of the m-th value of A_g, see Eq. (2), while $P(edp_i|a_{g,m})$ is the POE of the i-th value of the *EDP* conditioned on $A_g = a_{g,m}$. The probability of occurrence of the i-th threshold of the *EDP* is given by its POE as follows:

$$p(edp_i) = P(edp_i) - P(edp_{i+1}) \tag{11}$$

At higher intensity levels of the seismic hazard, it is likely to observe global collapse. In PEER PBEE, global collapse is treated separately since its probability does not change for different damageable groups (Günay and Mosalam, 2013). A realistic representation of the global collapse can be obtained through a progressive collapse algorithm (Talaat and Mosalam, 2007; Talaat and Mosalam, 2009). A practical method to determine global collapse is to determine the collapse seismic capacity edp_C of a representative parameter, e.g. interstory drift, and evaluate the corresponding probabilities of global collapse $p(C|a_{g,m})$ and of no collapse $p(NC|a_{g,m})$ conditioned on $A_g = a_{g,m}$. The probabilities of global collapse $p(C)$ and of no collapse $p(NC)$ are obtained by summing the conditional probability of collapse over the return periods as follows:

$$\begin{cases} p(C) = \sum_m P(C|a_{g,m})p(a_{g,m}) \\ p(NC) = 1 - p(C) \end{cases} \tag{12}$$

All the probabilities described in Eqs. (10)-(12) can be determined through tools of stochastic dynamic analysis, or approaches based on statistics and machine learning tools. Typically, in PEER PBEE, a LN distribution is adopted to fit the data. In this paper, we adopt the KDMEM, which is a statistical approach based on the information theory, recently developed by the authors (Alibrandi and Mosalam, 2017c) and is briefly presented below for the sake of completeness.

2.2.1 Kernel Density Maximum Entropy (KDMEM)

It is assumed that n_s artificial accelerograms have been simulated for chosen $a_{g,m}$, and n_s peak values of the *EDP* are subsequently available. The target PDF, $f_{EDP}(edp)$, is expressed as a linear

superposition of Kernel Density Functions (KDFs) as follows:

$$f_{EDP}(edp) \cong f_{KD}(edp) = \sum_{i=1}^{N} p_i f_{EDP}^{G}(edp; edp_i, \sigma) \tag{13}$$

where the coefficients p_i satisfy the constraints $0 \le p_i \le 1$, $\sum_i p_i = 1$, while $f_{EDP}^{G}(edp; edp_i, \sigma)$ is the i-th basis KDF, here assumed Gaussian, centered in edp_i with standard deviation σ, i.e.

$$f_{EDP}^{G}(edp; edp_i, \sigma) = \frac{1}{\sigma\sqrt{2\pi}} exp\left\{-\frac{1}{2}\left(\frac{edp - edp_i}{\sigma}\right)^2\right\} \tag{14}$$

The centers edp_i, i = 1, 2, ..., N, are uniformly spaced with a constant step $\Delta edp = edp_{i+1} - edp_i$ in the range $[edp_{min}, edp_{max}]$. The standard deviation is $\sigma = (2/3)\Delta edp$, which is shown to be a suitable value under uniform spacing of the centers (Alibrandi and Ricciardi, 2008; Alibrandi and Mosalam, 2017c). It is noted that when $N \to \infty$, then $\sigma \to 0$, and Eq. (13) gives

$$f_{KD}(edp) = \sum_{i=1}^{N} p_i \delta(edp - edp_i) \tag{15}$$

where δ is the Dirac delta function. Therefore, the representation (13)-(15) can reconstruct any kind of distribution. Multiplying both sides of Eq. (15) by edp^{α_k}, α_k being positive real number, $k = 1, 2, \ldots, M$, and integrating over the domain, the following relationship holds:

$$\begin{cases} \sum_{i=1}^{N} p_i = 1 \\ \sum_{i=1}^{N} M_{ki}(\boldsymbol{\alpha}) p_i = \mu_i(\alpha), k = 1, 2, \ldots, M \end{cases} \tag{16}$$

where

$$\begin{aligned} M_{ki}(\boldsymbol{\alpha}) &= \int_0^{\infty} exp^{\alpha_k} \delta(edp - edp_i) d(edp) = edp_i^{\alpha_k} \\ \mu_k(\boldsymbol{\alpha}) &= \int_{\Omega_z} edp^{\alpha_k} f_{EDP}(edp) d(edp) = E[EDP^{\alpha_k}] \end{aligned} \tag{17}$$

In Eqs. (16)-(17), $\mu_k(\boldsymbol{\alpha})$ collects the first M fractional moments (Novi Inverardi and Tagliani, 2003; Taufer *et al*., 2009; Zhang and Pandey, 2013) of the *EDP*, which have some attractive properties with respect to the classical power moments. First, the fractional moments can be defined for low values of $\alpha \le 2$, such that the estimates of sample fractional moments derived from a small sample of n_s data can be robust enough. Second, a reduced number of fractional moments gives the same information of several power moments, such that just M = 4 fractional moments may provide a good description of the tails. The free parameters $p_1, p_2, \ldots, p_N$, appearing in Eq. (16), are obtained through the maximization of the Shannon's entropy $H(\boldsymbol{p}) = -\sum_{i=1}^{N} p_i ln(p_i)$ as follows:

$$\begin{cases} \max_{\boldsymbol{p}} H(\boldsymbol{p}) \\ \sum_{i=1}^{N} p_i = 1 \\ \sum_{i=1}^{N} M_{ki}(\boldsymbol{\alpha}) p_i = \mu_k(\boldsymbol{\alpha}), k = 1, 2, \ldots, M \end{cases} \tag{18}$$

where p collects the N free parameters $p_1, p_2, \ldots, p_N$. The convexity of the optimization problem (18) implies the uniqueness of the MaxEnt (ME) solution $\boldsymbol{p}_{ME}$, which, according to Jaynes (Jaynes, 1957; Jaynes, 1968), is the least biased distribution, given the satisfaction of the available information. The substitution of $\boldsymbol{p}_{ME}$ into Eq. (13) gives the KDME PDF $f_{KDME}(edp)$.

2.2.2 Credible Bounds of KDME for Given Sample of Data

The number n_s of artificial accelerograms required by the seismic codes is typically low (less than 20). Thus, it is of interest to investigate the incurred error. To this aim, credible bounds of the KDME distribution are determined through the bootstrap resampling (Efron, 1982). Assume that a sample of size n_s = 5 of a chosen *EDP* has been determined (e.g. maximum interstory drift expressed in percent) such that $EDP = \{2.5, 2.2, 1.8, 2.6, 2.1\}$, which are drawn from the unknown distribution $F_{EDP}(edp)$. It is assumed that the sample represents the bootstrap population, whose distribution is modeled through a uniform discrete-valued distribution. Thus, each value of the sample has a probability of occurrence $\hat{p}_{EDP}^{(B)}(EDP = edp^{(i)}) = 1/n_s$, $i = 1, 2, \ldots, n_s$, i.e. $\hat{p}_{EDP}^{(B)}$ (EDP = 2.5%) = $\hat{p}_{EDP}^{(B)}(EDP = 2.5\%) = \hat{p}_{EDP}^{(B)}(EDP = 2.2\%) = \cdots =$ 1/5.

From the bootstrap discrete distribution $\hat{p}_{EDP}^{(B)}$, the bootstrap CDF $\hat{F}_{EDP}^{(B)}(edp)$ is determined. Bootstrap samples $EDP_{(B)}^{(s)}$ of size n_s can be so drawn from $\hat{F}_{EDP}^{(B)}(edp)$. The elements of $EDP_{(B)}$ are the same as those of the original data set, but repetitions may occur, i.e. some elements may appear only once, some may appear two or more times, and others may not appear. For illustration, two possible bootstrap samples are $EDP_{(B)}^{(1)} = \{2.5, 2.2, 2.2, 2.6, 1.8\}$ and $EDP_{(B)}^{(2)} \equiv \{2.2, 2.1, 1.8, 2.6, 1.8\}$. For the s-th bootstrap sample, $EDP_{(B)}^{(s)}$, $s = 1, 2, \ldots, S$, the KDME CDF is evaluated as $F_{KDME}^{(s)}(edp) = \sum_{i=1}^{N} p_i^{(s)} F_{EDP}^{G}(edp)$. It is noted that $P_{KDME}^{(s)}(edp) = 1 - F_{KDME}^{(s)}(edp) = Prob[EDP^{(s)} \ge edp]$. Therefore, S bootstrap samples provide S different values of $P_{KDME}(edp)$, and the corresponding bootstrap distribution $P_{KDME}^{(B)}(edp)$ is determined. From $P_{KDME}^{(B)}(edp)$, the bootstrap confidence intervals can be determined by choosing two percentiles for lower bound (LB), q_{LB}, and upper bound (UB), q_{UB}, of $P_{KDME}^{(B)}(edp)$.

The knowledge of the confidence intervals is beneficial for risk-informed decision(s). This is known to be the case since several studies have shown that the decision makers prefer a statement of confidence in the risk assessment, with particular reference to low-probability high-consequence events (Building Seismic Safety Council, 2009; Ellingwood and Kinali, 2009).

2.3 Damage Analysis

The damage analysis estimates the physical damage at the component or system levels as a function of the structural response. Typically, the damage measures are defined in terms of damage levels corresponding to repair measures needed to restore the components of a facility to the original conditions. In the PEER PBEE framework, the focus of the damage analysis is to evaluate for each damageable group the "fragility function," which is the POE of a *DM* for different values of an *EDP*.

Typically, the facility is divided into damageable groups affected by the same *EDP* in a similar manner, e.g. structural elements, drift-sensitive and acceleration-sensitive non-structural elements. The POE of the damage measures are given as follows:

$$P(dm_j) = Prob[DM \geq dm_j] = \sum_i P(dm_j|edp_i)p(edp_i) \quad (19)$$

where $P(dm_j|edp_i)$ is the POE of the j-th value of DM conditioned on $EDP = edp_i$, while $p(edp_i)$ is the probability of occurrence of the i-th value of EDP. The probability of occurrence of the j-th threshold of DM is given by

$$p(dm_j) = Prob[dm_j \leq DM \leq dm_{j+1}] = P(dm_j) - P(dm_{j+1}) \quad (20)$$

Typically, the damage measure is expressed in terms of a number discrete of damage states, e.g. No damage ($dm_0 = 0$), Slight (dm_1), Moderate (dm_2), Extensive (dm_3) and Complete (dm_4). In view of Eq. (20), the probability of no damage is $p(dm_0) = Prob[0 \leq DM \leq dm_1]$, Slight damage has probability $p(dm_1) = Prob[dm_1 \leq DM \leq dm_2]$, and so on.

2.4 Loss Analysis

In the final stage of the PEER PBEE methodology, the damage is converted to the *DVs*. These variables can be used directly by the designers in the design process with inclusion of stakeholders for the decision-making process. Some commonly utilized decision variables are Economic Loss, Functionality Loss, Fatalities, and Downtime. However, the definition of *DV* is broad and it can denote performances also in terms of resilience and sustainability (Alibrandi and Mosalam, 2017a; Mosalam *et al*., 2018). The POE of the chosen *DV* reads as follows:

$$P(dv_q) = Prob[DV \geq dv_q] = \sum_j P(dv_q|dm_j)p(dm_j) \quad (21)$$

where $P(dv_q|dm_j)$ is the POE of the q-th value of DV conditioned on $DM = dm_j$, i.e. $P(dv_q|dm_j) = Prob(DV \geq dv_q|DM = dm_j)$, while $p(dm_j)$ is the probability of occurrence of the j-th damage state.

3. Application Example

A hypothetical four-bay, five-story Reinforced Concrete (RC) office building in Italy is analyzed. The building is regular in plan and elevation. Its plan dimensions are 20 × 20 m, while the spacing of the columns is 5 m. The total area at each floor is A_f = 400 m^2, while the total building area is A = 5 × 400 = 2,000 m^2. The total height of the building is 20 m with floor-to-floor height equal to 4 m. Given the symmetry of the building, a two-dimensional model is adopted, refer to Fig. 1. All the beam and column sections are 300 × 500 mm with 8 reinforcing bars of 16 mm diameter. The fundamental period of the frame is T_1 = 1.04 sec, and its fundamental frequency is $\omega_1 = 2\pi/T_1$ = 5.99 rad/sec. The construction cost is assumed c_0 = 1,200 €/m^2, for a total amount of C_0 = 1,200 × 2,000 = 2.4 €M.

3.1 Code-Conforming Stochastic Seismic Hazard Analysis

The building is located in Messina, Italy, whose latitude and longitude are respectively 15.522° and 38.216°. The Eurocodes EC8 (Eurocode, 2004), Italian Annex (NTC08, 2008) is adopted. The elastic acceleration response spectrum is as follows:

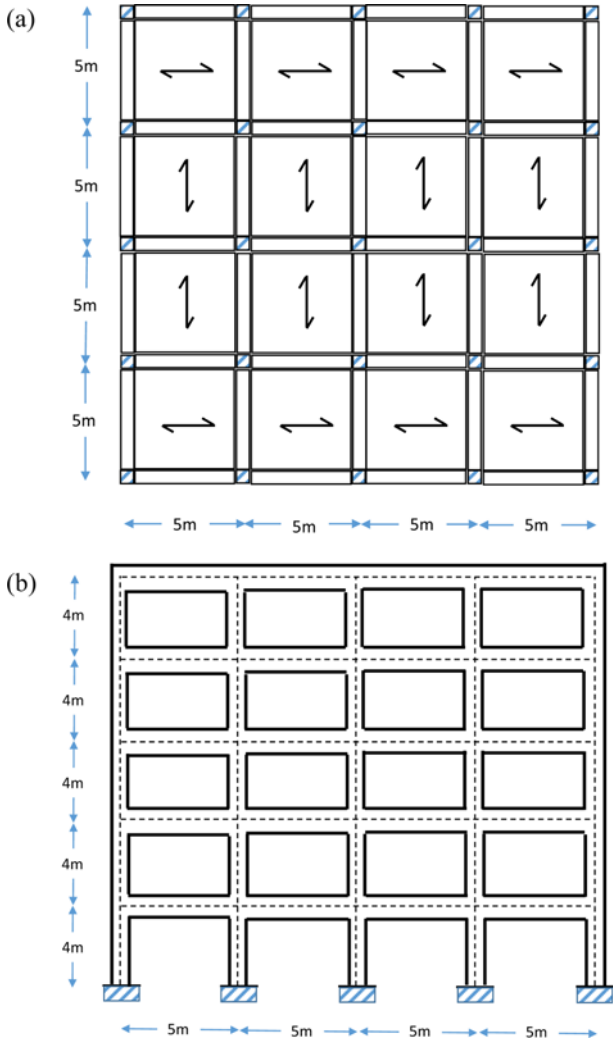

Fig. 1. Schematic of the Model of an Office Building in Italy: (a) Plan, (b) 2D Frame

$$RSA(T,\zeta_0) = \begin{cases} a_g S \eta F_0 \left[\frac{T}{T_B} + \frac{1}{\eta F_0}\left(1 - \frac{T}{T_B}\right)\right] & 0 \leq T \leq T_B \\ a_g S \eta F_0 & T_B \leq T \leq T_C \\ a_g S \eta F_0 \left(\frac{T_C}{T}\right) & T_C \leq T \leq T_D \\ a_g S \eta F_0 \left(\frac{T_C T_D}{T^2}\right) & T_D \leq T \leq T_E \end{cases} \quad (22)$$

where $\eta = \sqrt{10/(5+100\zeta_0)}$ is the damping correction factor, F_0 is the peak spectral amplification, S is the soil factor, T_B and T_C are respectively the lower and upper limits of the period of the constant spectral acceleration branch, T_D and T_E = 4 sec are respectively the values defining the beginning and end of the constant displacement response range of the spectrum. The beginning of the branch of the spectrum with constant velocity is

Table 1. Seismic Parameters of the Elastic Acceleration Response Spectrum, in Messina, Italy

T_R	30	50	72	101	140	201	475	975	2,475
a_g[g]	0.058	0.078	0.095	0.114	0.134	0.160	0.238	0.324	0.470
F_0	2.39	2.34	2.33	2.33	2.35	2.37	2.41	2.44	2.49
T_C^*	0.28	0.30	0.31	0.32	0.33	0.34	0.36	0.38	0.43

denoted by T_C^*. The Italian codes provide for each location the values of A_g, F_0 and T_C^* in terms of the return period T_R. In Table 1, specific values related to the considered geographic location are listed. The periods T_B, T_C and T_D are defined as follows:

$$\begin{cases} T_B = \dfrac{T_C}{3} \\ T_C = C_C T_C^* \\ T_D = 4\dfrac{a_g}{g} + 1.6 \end{cases} \tag{23}$$

where C_C depends on T_C^* and the soil type. The soil factor is defined as $S = S_S \cdot S_T$, where S_S and S_T take into account the soil type and the topographic amplification, respectively. It is assumed that the soil type is "*B*," while the foundation ground has a slope i <15° (S_T = 1).

The response spectra drawn from the return periods described in Table 1 are shown in Fig. 2. It is seen that for increasing return periods of the seismic event, the intensity and the spectral shape of the response spectrum change. In Fig. 3, the seismic hazard curve in terms of A_g is shown where the circle markers denote the

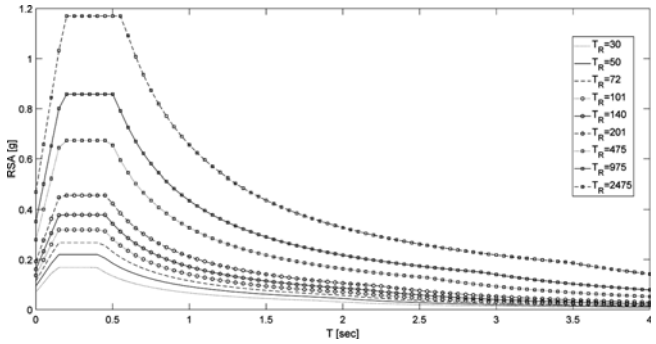

Fig. 2. Elastic Acceleration Response Spectra for Different Intensity Levels of the Seismic Event

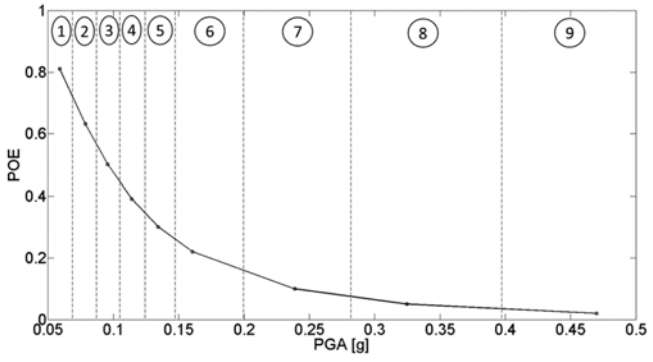

Fig. 3. Seismic Hazard Curve

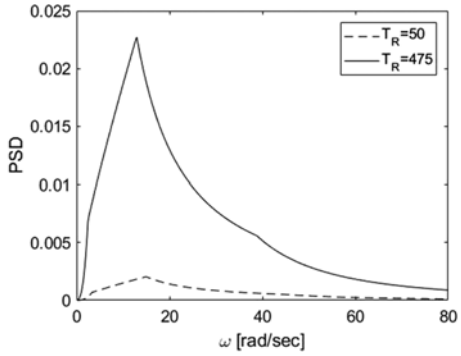

Fig. 4. PSD Coherent with the Elastic Acceleration Response Spectra for T_R = 50 and 475 years

points $a_{g,1}, a_{g,2}, \ldots, a_{g,9}$ represented in Table 1, while the dashed lines denote the striping $a_{g,1}^U, a_{g,2}^U, \ldots, a_{g,8}^U$ to be used for time-based assessment. The PGA $a_{g,m}$ represents the center of each stripe, such that $a_{g,m-1}^U \le a_{g,m} \le a_{g,m}^U$. The application of Eq. (2) gives $p(a_{g,m}^U) = Prob[a_{g,m-1}^U \le A_g \le a_{g,m}^U]$, $m = 2, 3, \ldots, 8$, while $p(a_{g,1}^U) = Prob[A_g \le a_{g,1}^U]$ and $Prob[A_g \ge a_{g,8}^U] = 1 - \sum_{m=1}^{8} p(a_{g,m}^U)$. The second step of the hazard analysis is the selection of a set of ground motions compatible with the hazard curve. Here, artificial accelerograms compatible with the response spectrum are simulated. At first, stationary accelerograms are simulated since they are allowed by the codes, and they are widely employed in engineering practice. To this aim, the Power Spectral Densities (PSD), $G_{A_g}(\omega)$, coherent with the chosen nine acceleration response spectra are determined, see Eqs. (3) and (5)-(9). In Fig. 4, these PSDs for T_R = 50 and 475 years are shown. In the Italian codes, these return periods are of particular interest and they are defined as representative of the Service Limit State (SLS) and Ultimate Limit State (ULS), respectively. Stationary artificial accelerograms are simulated through Eq. (4) where the evolutionary PSD is assumed coinciding with the stationary PSD, i.e. $G_{A_g}(t, \omega) \equiv G_{A_g}(\omega)$. Here we have assumed t_{fim} = 30 sec with time step Δt = 0.02 sec. The maximum frequency is ω_c = 80rad/sec , with $\Delta\omega = (2\pi)/t_{fin}$ = 0.209 rad/sec.

3.2 Structural Analysis

The structural analyses are developed using the software OpenSees (McKenna, 2010). Beams and columns are modeled using displacement-based beam-column elements with fiber discretized sections. Core and cover concrete are modeled using *Concrete01* with compressive strength of 35 MPa, and strains at maximum strength and at crushing strength as 0.2% and 0.5%, respectively. The reinforcing bars are modeled with *Steel01* with yield strength of 420 MPa, elastic modulus of 200,000 MPa, and

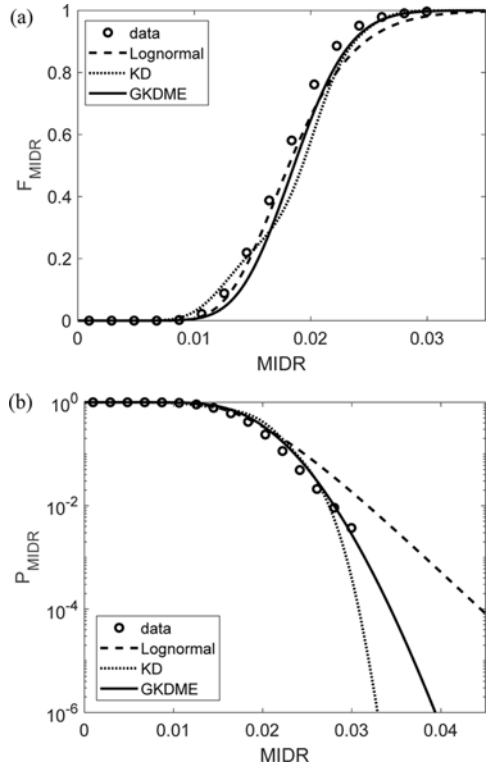

Fig. 5. Fragility Curve of the MIDR Given a Seismic Event for T_R = 475 years. Comparison of MCS (100,000 samples) with KD, KDME and LN (20 samples) in Terms of: (a) CDF, (b) POE in Semi-logarithmic Scale

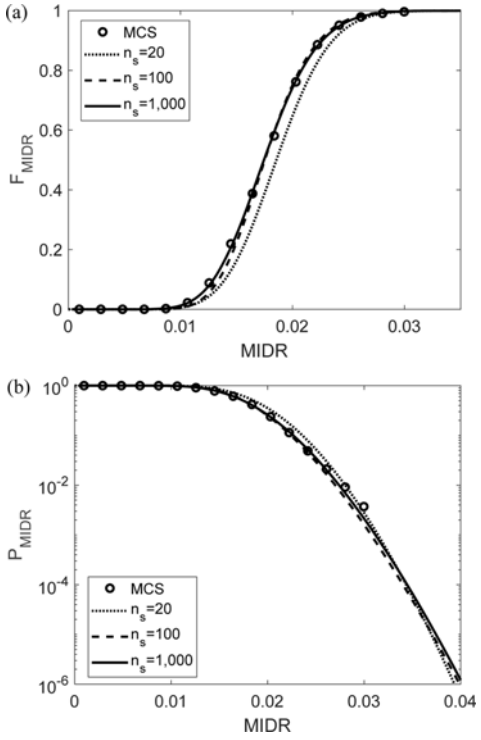

Fig. 7. Fragility Curve of the MIDR Given a Seismic Event for T_R = 475 years. Comparison of MCS (100,000 samples) with KDME Model Trained using 20, 100 and 1,000 Samples, in terms of (a) CDF, (b) POE in Semi-logarithmic Scale

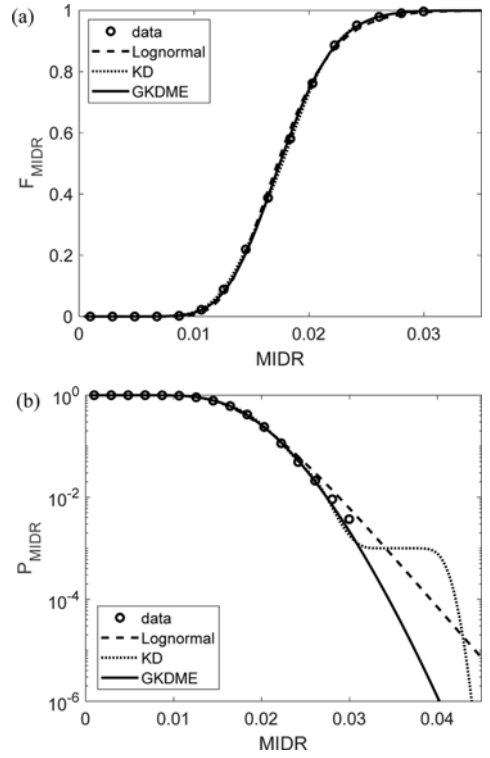

Fig. 6. Fragility Curve of the MIDR Given a Seismic Event for T_R = 475 years. Comparison of MCS (100,000 samples) with KD, KDME and LN (1,000 samples) in Terms of: (a) CDF, (b) POE in Semi-logarithmic Scale

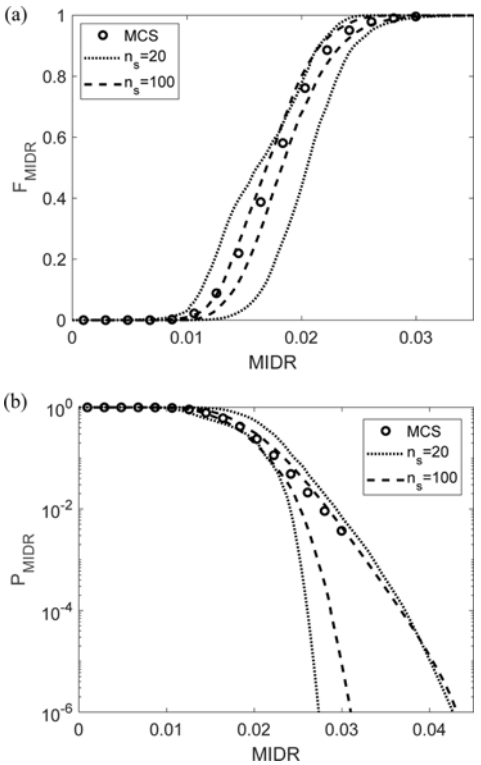

Fig. 8. Fragility Curve of the MIDR Given a Seismic Event for T_R = 475 years. Comparison of MCS (100,000 samples) with Credible Bounds of KDME using 20 and 100 Samples, in Terms of (a) CDF, (b) POE in Semi-logarithmic Scale

strain hardening ratio $b = 0.05$. For simplicity, in this paper, the only EDP considered is the Maximum Interstory Drift Ratio (MIDR).

The fragility curves are determined through KDMEM, whose good properties of accuracy and efficiency have already been shown in (Alibrandi and Mosalam, 2017c). Here it is underlined that for high number of kernel densities, in view of Eq. (15), the KDME PDF converges to the MaxEnt distribution, which is the "most honest distribution given the available information" (Jaynes, 1968) since it "assumes the least" about the distribution itself. As a consequence, the information theory guarantees that for a given number of ground motions, KDMEM provides the least biased seismic fragility curve. Moreover, since in the optimization problem (18) fractional moments are adopted as constraints, KDMEM is able to guarantee good approximations also in the tail region (Xu, 2016; Xu *et al*., 2016; Zhang and Pandey, 2013; Alibrandi and Mosalam, 2017c). To show the performances of KDMEM inside the proposed framework, the seismic fragility curves for a return period $T_R = 475$ years are represented in Figs. 5 and 6. Here three probability models are adopted: (*i*) a LN distribution (dashed line), as typically done in PBEE, (*ii*) Kernel Density estimation (dotted line), and (*iii*) KDME approach (continuous line), The models are compared with Monte Carlo Simulation (MCS) using 100,000 samples (circle markers). In Figs. 5 and 6, the statistical models are trained using 20 and 1,000 samples, respectively. It is seen that: (*i*) KD and KDME are data-driven distributions, and their accuracy improves when the number of sampling points increases, (*ii*) KDME has good capabilities of prediction over the tails, differently from LN and KD distributions, (*iii*) the LN fit provides overconservative estimates in the tail region. In Fig. 7, the good convergence properties of KDME are shown, by comparing the approximations provided using $n_s = 20$, 100 and 1,000 artificial ground motions. It is seen that $n_s = 100$ samples provide an adequate estimate of the whole distribution, including its tails. Finally, in Fig. 8 the credible bounds of the KDME PDFs are presented using $n_s = 20$ and $n_s = 100$.

The fragility seismic curves $F[MIDR|PGA]$ are determined for different values of PGA, and using Eq. (10) the distribution F(MIDR) is determined. In Fig. 9, the KDME model trained with $n_s = 20$ artificial accelerograms is shown, together with its credible bounds. When the number of ground motions increases, the bounds become narrower.

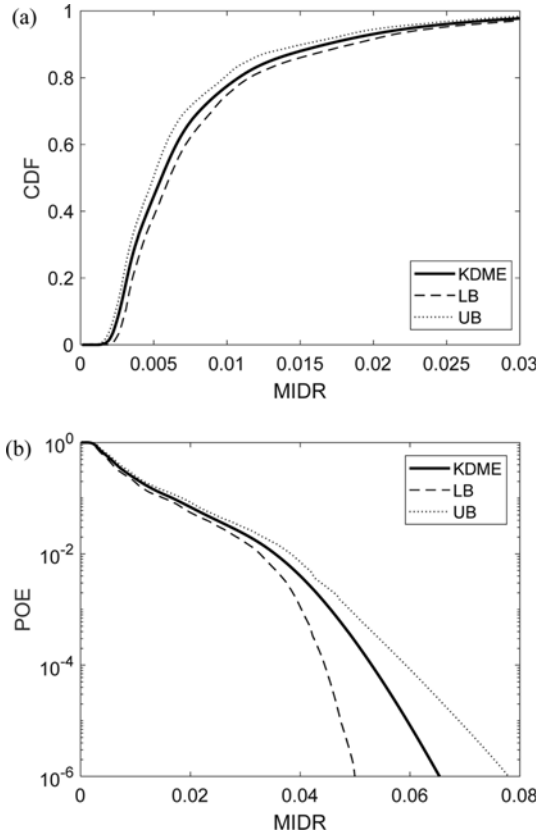

Fig. 9. Cumulative Distribution of MIDR Trained using 20 Artificial Accelerograms: (a) Arithmetic Scale, (b) POE in Semilogarithmic Scale

3.3 Damage Analysis

The *DM* is assumed coincident with the *MIDR*. Four damage states are considered: Slight, Moderate, Extensive, and Complete. In the definition of the fragility curves, the seismic capacities play a significant role. They are modeled as random variables following LN distributions whose median values of the *MIDR* are $edp_1 = 0.33\%$, $edp_2 = 0.58\%$, $edp_3 = 1.56\%$ and $edp_4 = 4.00\%$. These values are based on HAZUS (FEMA, 2013), because of the absence of available data. The dispersion value is assumed to be 0.3. The collapse value of the *MIDR* is assumed to follow a LN distribution whose median value is $edp_C = 6.6\%$ with a coefficient of variation $COV = 0.30$. The damage states are therefore defined as: None ($DS_0 \equiv [0, edp_1]$), Slight ($DS_1 \equiv [edp_1, edp_2]$), Moderate ($DS_2 \equiv [ed(p_2, edp_3)]$), Extensive ($DS_3 \equiv [edp_3, edp_4]$) and Complete ($DS_4 \equiv [edp_4, edp_C]$). To evaluate the probability of damage, MCS is adopted. From the knowledge of $F(MIDR)$, a sample $MIDR^{(k)}$ is simulated, together with the values of the seismic capacities $edp_1^{(k)}, dep_2$,

Table 2. Probability of Occurrence of the Damage States using the KDME Model, Trained using 20, 100 and 1,000 Stationary Artificial Accelerograms

Model	None	Slight	Moderate	Extensive	Complete	Collapse
KDME $n_s = 20$	0.234	0.292	0.353	0.111	0.99×10^{-2}	0.73×10^{-3}
KDME $n_s = 100$	0.225	0.284	0.354	0.113	1.13×10^{-2}	1.21×10^{-3}
KDME $n_s = 1{,}000$	0.224	0.289	0.356	0.116	1.17×10^{-2}	1.61×10^{-3}

$edp_3^{(k)}, edp_4^{(k)}$, and $edp_C^{(k)}$. In this way, it is determined to which damage state the sample belongs.

The probability of occurrence of the damage states are given as $p(DM = DS_k) = N_{DS_k}/N$, where N = 1,000,000 is the number of simulated samples, while N_{DS_k} is the number of samples belonging to the damage state DS_k.These probabilities are listed in Table 2 for the KDME model, trained using n_s = 20, 100 and 1,000 ground motions. From this table, it can be observed that 20–100 ground motions may suffice to achieve good estimates of the damages.

3.4 Loss Analysis

The loss functions are derived from HAZUS, which suggests to adopt as repair costs 0.4%, 1.9%, 9.6% and 19.2% of the replacement cost of the building for the damage states DS_1, DS_2, DS_3 and DS_4, respectively. These values provide 9,600 €, 45,600 €, 230,400 € and 460,800 € for the four damage states. They are assumed as median values of the probability distributions $P[L|DM = DS_k]$, k = 1, 2, 3, 4 following LN distributions whose dispersion is assumed to be 0.3. It is also assumed that the loss given the collapse event follows LN distribution, whose median is 2,688,000 € (112% of the replacement cost) and COV = 0.30. In Fig. 10, the losses curve $P_L(l)$ is shown, together with its bounds using n_s = 20 ground motions. The expected cost $E[L]$ during the lifecycle T_L is a commonly used metric for risk-informed decision making. In (Yang *et al*., 2006), it is shown that $E[L]$ is given by the area underlying the curve $P_L(l)$, i.e.

$$E[L] = \int_0^\infty P_L(l)dl \tag{24}$$

It is underlined that this value considers only the losses due to the seismic damage during the lifecycle where degradation of the materials, operation and maintenance costs are not included. In Table 3 the values of the expected cost, including their bounds are summarized for n_s = 20, 100 and 1,000 ground motions.

3.5 Model Uncertainty

To consider the uncertainty related to the earthquake model, some nonstationary models have been explored. First, two

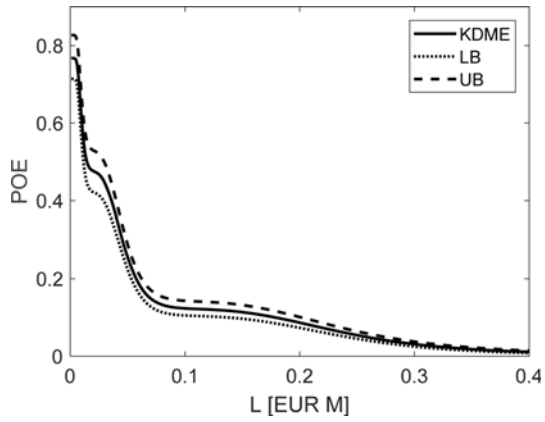

Fig. 10. Loss Curve Trained using 20 Artificial Accelerograms

Table 3. Expected Costs, Including Their Bounds, using the KDME Model, Trained using 20, 100 and 1,000 Stationary Artificial Accelerograms.

Model	LB [€]	EC[€]	UB [€]
KDME n_s = 20	45,336	53,121	61,409
KDME n_s = 100	50,678	55,655	61,755
KDME n_s = 1,000	55,994	57,702	59,459

different time-dependent modulating functions are considered: the model $\varphi_{HB}(t)$ proposed by Hsu and Bernard (Hsu and Bernard, 1978)

$$\varphi_{HB}(t) = \varepsilon_{HB} t exp(-\mu_{HB} t) \tag{25}$$

where

$$\mu_{HB} = \frac{1}{t_{max}}[sec^{-1}], \varepsilon_{HB} = \frac{exp(1)}{t_{max}}[sec^{-1}] \tag{26}$$

with t_{max} = 5 sec and the modulating function $\varphi_J(t)$ of Jennings (Jennings *et al*., 1969)

$$\varphi_J(t) = \begin{cases} \left(\frac{t}{t_{1,J}}\right)^2 & t < t_{1,J} \\ 1 & t_{1,J} \le t \le t_{2,J} \\ exp[-\beta_J(t - t_{2,J})] & t > t_{2,J} \end{cases} \tag{27}$$

The parameters of $\varphi_J(t)$ are obtained by imposing that at time instants $t_{1,J}$ and $t_{2,J}$, the energy of the stochastic ground motion is equal to 5% and 95%, respectively. Following (Cacciola *et al*., 2014) one has the following:

$$t_{1,J} = \frac{2.5}{\beta_J}[\text{sec}],\ t_{2,J} = \frac{11.5}{\beta_J}[\text{sec}] \tag{28}$$

In the numerical application, β_J = 0.9 is chosen, which provides $t_{1,J}$ = 2.78 sec and $t_{2,J}$ = 12.78 sec. Moreover, a model fully nonstationary is considered by adopting the time-frequency modulating function of Solomos & Spanos $\varphi_{SS}(t, \omega)$ (Spanos and Solomos, 1983)

$$\varphi_{SS}(t, \omega) = \varepsilon_{SS}(\omega) t\ exp[-\mu_{SS}(\omega) t] \tag{29}$$

where

$$\varepsilon_{SS}(\omega) = \frac{1}{2t_{max}}\left[1 + \left(\frac{\omega}{\omega_{max}}\right)^2\right][\text{sec}^{-1}], \mu_{SS}(\omega) = \frac{\omega\sqrt{2}}{15\pi}[\text{sec}^{-1}] \tag{30}$$

In the numerical application, t_{max} = 6.67 sec and ω_{max} = 12.89 red/sec have been chosen. In Figs. 11 the three discussed modulating functions are presented, while in Fig. 12 some artificial accelerograms simulated through Eq. (4) for the return period of T_R = 475 years are shown. Here four different models are considered: stationary (S), the two different quasi-stationary models based on the modulating functions of Hsu-Bernand (QSHB) and Jennings (QSJ), and the nonstationary (NS) model based on the function of Solomos and Spanos. In Figs. 13 and 14 we represent the seismic fragility curves for the return periods T_R

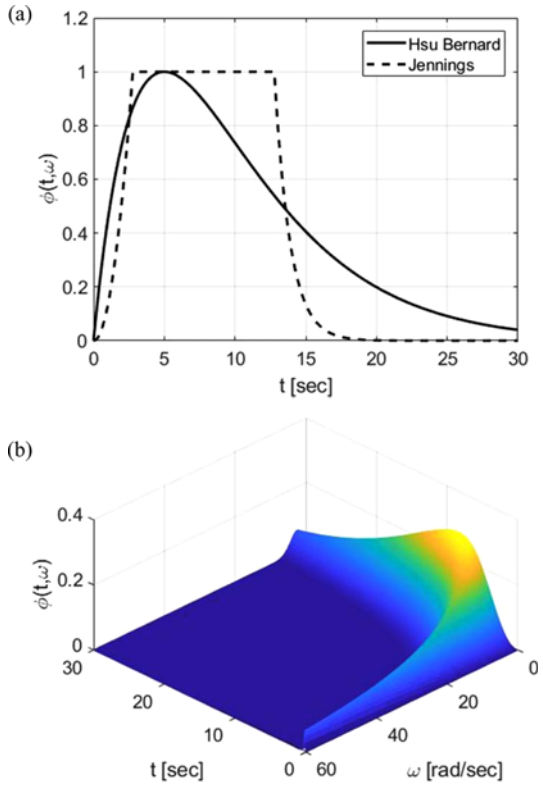

Fig. 11. Modulating Functions, (a) Time-dependent Models, (b) Time-frequency Models

= 50 and T_R = 475 years, corresponding in the Italian codes, to the Service Limit State (SLS) and Ultimate Limit State (ULS). Typically for SLS, the structure has linear behavior, while for ULS is designed to behave inelastically. The curves show that for both linear and non-linear behavior, the stationary accelerograms may not provide conservative results for frequent events, while they are always on the unsafe side for low-probability high-consequence events. The effects of the model uncertainty are of course propagated also into the probability of occurrence of the damage states and economic losses, summarized in Table 4.

4. Conclusions

The Performance-Based Earthquake Engineering (PBEE) approach is a powerful tool for the analysis of structures subjected to seismic excitation in a rigorous probabilistic manner. One of the key features of Pacific Earthquake Engineering Research (PEER) Center PBEE is the explicit calculation of system performance measures, e.g. monetary losses, downtime, and casualties, which are expressed in terms of the direct interest of various stakeholders. Currently, the PEER PBEE methodology can be used to: (*i*) evaluate a traditional code-based design in a performance-based probabilistic approach, (*ii*) evaluate the performance of an existing structure, and (*iii*) adopt the methodology for decision-making amongst different design alternatives. In this paper, the

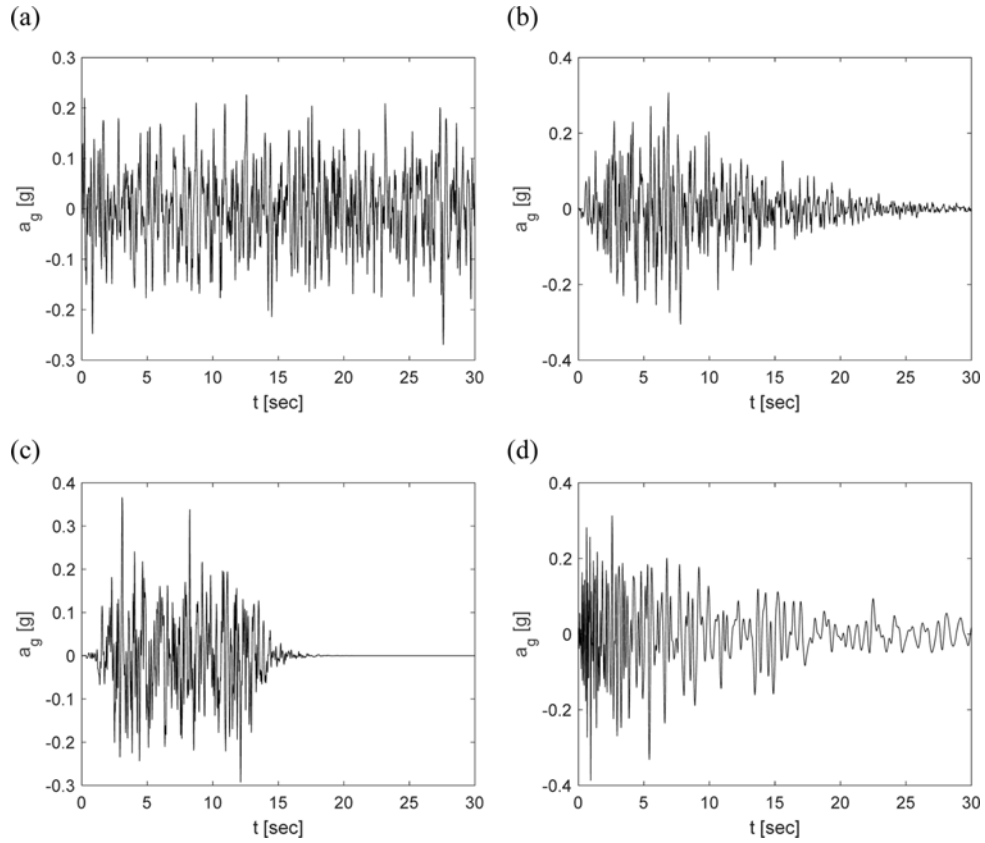

Fig. 12. Artificial Accelerograms Coherent with the Elastic Acceleration Response Spectra for T_R = 475 years: (a) Stationary Model, (b) Quasi Stationary Model of Hsu-Bernard, (c) Quasi Stationary of Jennings, (d) Non-stationary Model

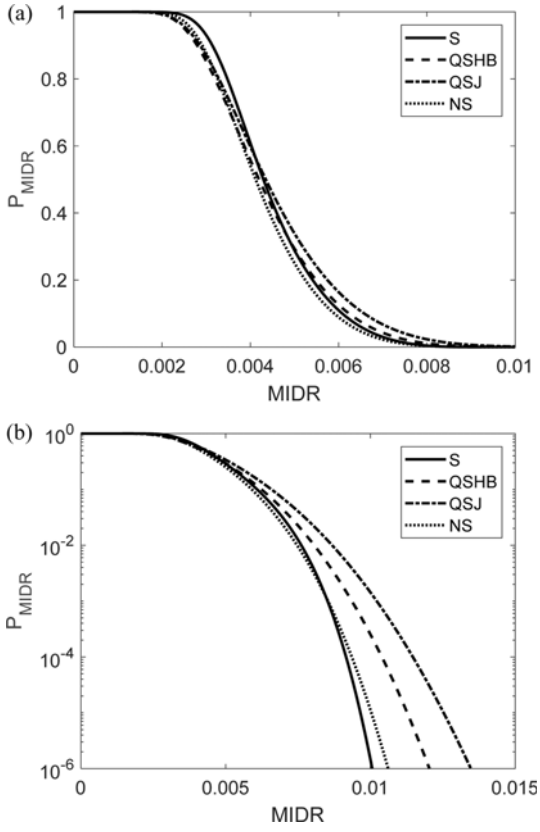

Fig. 13. Fragility Curve of the MIDR Given a Seismic Event for T_R = 50 years. Comparison of the POE of Different Stochastic Ground Motion Models, in Scale: (a) Arithmetic, (b) Semi-logarithmic Scale

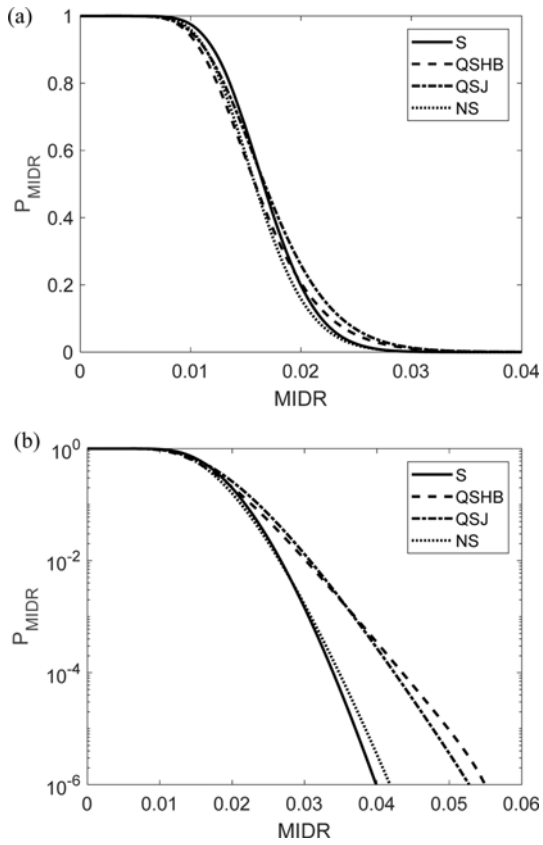

Fig. 14. Fragility Curve of the MIDR Given a Seismic Event for TR = 475 years. Comparison of the POE of Different Stochastic Ground Motion Models, in Scale: (a) Arithmetic, (b) Semi-logarithmic Scale

PEER PBEE is considered by adopting the tools of the stochastic dynamic analysis and information theory. The proposed approach has several important features. First, it allows to apply the PEER PBEE approach to a seismic excitation compatible with code-conforming response spectra, such that it can be adopted as a practical tool for design in current engineering practice. The proposed stochastic model does not require the engineer to develop probabilistic seismic hazard analysis, including selection of ground motions, and scaling. Therefore, engineers can design by using the mandatory codes and develop performance-based engineering analyses. Accordingly, the proposed approach fills the gap between the classical code-conforming designs and the enhanced performance-based designs.

The stochastic response is evaluated in this study through the recently proposed Kernel Density Maximum Entropy Method (KDMEM), which allows to determine, with a reduced number of artificial ground motion (say 20-100), the distribution of each quantity of interest. It is a data-driven statistical approach, such that its accuracy improves when the number of analyses increases. Moreover, it is based on the Maximum Entropy principle, such that for a chosen number of simulated ground motions, it provides the least biased and honest distribution given the available information.

The studied numerical example shows that the Power Spectral Density (PSD) fitting process (model and parameters) may determine not negligible model uncertainties. A comparison between stationary and non-stationary accelerograms shows that the stationary

Table 4. Probability of Occurrence of the Damage States and Expected Costs, using the KDME Model, Trained using 1,000 Artificial Accelerograms, Following Different Models of Generation: Stationary (S), Quasi-stationary with Function of Hsu-Bernard (QSHB) and Jennings (QSJ), and Fully Nonstationary (NS)

Model	Damage State						Expected Cost [€]
	None	Slight	Moderate	Extensive	Complete	Collapse	
S	0.224	0.289	0.356	0.116	1.17×10^{-2}	1.61×10^{-3}	57,702
QSHB	0.244	0.285	0.347	0.109	1.17×10^{-2}	2.30×10^{-3}	57,411
QSJ	0.228	0.285	0.356	0.115	1.29×10^{-2}	2.68×10^{-3}	61,034
NS	0.248	0.286	0.344	0.109	1.05×10^{-2}	1.40×10^{-3}	54,203

accelerograms provide unsafe responses for low-probability high-consequences events. In order to take into account the relevant epistemic uncertainties different stochastic ground motion models are adopted and included, while the risk-informed decision making process is supported through confidence intervals.

Acknowledgements

This research was funded by the Republic of Singapore's National Research Foundation through a grant to the Berkeley Education Alliance for Research in Singapore (BEARS) for the Singapore Berkeley Building Efficiency and Sustainability in the Tropics (SinBerBEST) program. BEARS has been established by the University of California, Berkeley, as a center for intellectual excellence in research and education in Singapore. Professor K.M. Mosalam is a principal investigator of Tsinghua-Berkeley Shenzhen Institute (TBSI). The authors acknowledge the funding support from SinBerBEST and the partial support from TBSI.

References

Alibrandi, U. (2014). "A response surface method for stochastic dynamic analysis." *Reliability Engineering & System Safety*, Vol. 126, pp. 44-53, DOI: 10.1016/j.ress.2014.01.003.

Alibrandi, U. and Mosalam, K. M. (2017a). "A decision support tool for sustainable and resilient building design." *Risk and Reliability Analysis: Theory and Applications*, Springer Series in Reliability Enigneering, pp. 509-536, DOI: 10.1007/978-3-319-52425-2_22.

Alibrandi, U. and Mosalam, K. M. (2017b). "Equivalent linearization methods for nonlinear stochastic dynamic analysis using linear response surfaces." *Journal of Engineering Mechanics*, Vol. 143, No. 8, DOI: 10.1061/(ASCE)EM.1943-7889.0001264.

Alibrandi, U. and Mosalam, K. M. (2017c). "The kernel density maximum entropy with generalized moments for evaluating probability distributions, including tails, from small sample of data." *International Journal for Numerical Methods in Engineering*, DOI: 10.1002/nme.5725.

Alibrandi, U. and Ricciardi, G. (2008). "Efficient evaluation of the pdf of a random variable through the kernel density maximum entropy approach." *International Journal for Numerical Methods in Engineering*, Vol. 75, No. 13, pp. 1511-1548, DOI: 10.1002/nme.2300.

Alibrandi, U., Ma, C., and Koh, C. G. (2016). "Secant hyperplane method for structural reliability analysis." *Journal of Engineering Mechanics*, Vol. 142, No. 3, DOI: 10.1061/(ASCE)EM.1943-7889.0001024.

Au, S. K. and Beck, J. L. (2001). "Estimation of small failure probabilities in high dimensions by subset simulation." *Probabilistic Engineering Mechanics*, Vol. 16, No. 4, pp. 263-277, DOI: 10.1016/S0266-8920(01)00019-4.

Basone, F., Cavaleri, L., Di Trapani, F., and Muscolino, G. (2017). "Incremental dynamic based fragility assessment of reinforced concrete structures: Stationary vs. non-stationary artificial ground motions." *Soil Dynamics and Earthquake Engineering*, Vol. 103, pp. 105-117, DOI: 10.1016/j.soildyn.2017.09.019.

Bucher, C. (2009). "Asymptotic sampling for high-dimensional reliability analysis." *Probabilistic Engineering Mechanics*, Vol. 24, No. 4, pp. 504-510, DOI: 10.1016/j.probengmech.2009.03.002.

Building Seismic Safety Council (2009). *NEHRP Recommended seismic provisions for new buildings and other structures,* Fema P-750, The Building Seismic Safety Council, Washington, D.C. Vol. II, p. 388.

Cacciola, P. (2010). "A stochastic approach for generating spectrum compatible fully nonstationary earthquakes." *Computers and Structures*, Vol. 88, Nos. 15-16, pp. 889-901, DOI: 10.1016/j.compstruc.2010.04.009.

Cacciola, P. and Zentner, I. (2012). "Generation of response-spectrum-compatible artificial earthquake accelerograms with random joint timefrequency distributions." *Probabilistic Engineering Mechanics*, pp. 52-58, DOI: 10.1016/j.probengmech.2011.08.004.

Cacciola, P., Colajanni, P., and Muscolino, G. (2004). Combination of Modal Responses Consistent with Seismic Input Representation: *Journal of Structural Engineering*, Vol. 130, No. 1, pp. 47, DOI: 10.1061/(ASCE)0733-9445(2004)130:1(47).

Cacciola, P., D'Amico, L., and Zentner, I. (2014). "New insights in the analysis of the structural response to response-spectrum-compatible accelerograms." *Engineering Structures*, Vol. 78, pp. 3-16, DOI: 10.1016/j.engstruct.2014.07.015.

Cornell, C. A. and Krawinkler, H. (2000). "Progress and challenges in seismic performance assessment." *PEER Center News*, Vol. 3, No. 2, pp. 1-4.

De Angelis, M., Patelli, E., and Beer, M. (2015). "Advanced Line Sampling for efficient robust reliability analysis." *Structural Safety*, Vol. 52, No. PB, pp. 170-182, DOI: 10.1016/j.strusafe.2014.10.002.

Efron, B. (1982). "The jackknife, the bootstrap and other resampling plans." *Complexity*, pp. 103, DOI: 10.1137/1.9781611970319.

Ellingwood, B. R. (2001). "Earthquake risk assessment of building structures." *Reliability Engineering & System Safety*, Vol. 74, No. 3, pp. 251-262, DOI: 10.1016/S0951-8320(01)00105-3.

Ellingwood, B. R. and Kinali, K. (2009). "Quantifying and communicating uncertainty in seismic risk assessment." *Structural Safety*, Vol. 31, No. 2, pp. 179-187, DOI: 10.1016/j.strusafe.2008.06.001.

EN 1998-1 (2004). "8: Design of structures for earthquake resistance—Part 1: General rules, seismic actions and rules for buildings." *European Committee for Normalization, Brussels*, Vol. 1, No. 2004.

FEMA (2013). *Earthquake model HAZUS*, MH Technical Manual.

FEMA ATC-58-1 (2011). "Seismic Performance Assessment of Buildings. Volume 1: Methodology." *Methodology*, Vol. 1, No. May.

Fujimura, K. and Der Kiureghian, A. (2007). "Tail-equivalent linearization method for nonlinear random vibration." *Probabilistic Engineering Mechanics*, Vol. 22, No. 1, pp. 63-76, DOI: 10.1016/j.probengmech.2006.08.001.

Grigoriu, M. (1993). "On the spectral representation method in simulation." *Probabilistic Engineering Mechanics*, Vol. 8, No. 2, pp. 75-90, DOI: 10.1016/0266-8920(93)90002-D.

Günay, S. and Mosalam, K. M. (2013). "PEER Performance-based earthquake engineering methodology, revisited." *Journal of Earthquake Engineering*, Vol. 17, No. 6, pp. 829-858, DOI: 10.1080/13632469.2013.787377.

Hsu, T.-I, and Bernard, M. C. (1978). "A random process for earthquake simulation." *Earthquake Engineering & Structural Dynamics*, Vol. 6, No. 4, pp. 347-362, DOI: 10.1002/eqe.4290060403.

Jaynes, E. T. (1957). "Information theory and statistical mechanics." *Physical Review*, Vol. 106, No. 4, pp. 620-630, DOI: 10.1103/PhysRev.106.620.

Jaynes, E. T. (1968). "Prior probabilities." *IEEE Transactions on Systems Science and Cybernetics*, Vol. 4, No. 3, pp. 227-241, DOI: 10.1109/TSSC.1968.300117.

Jennings, P., Housner, G., and Tsai, C. (1969). "Simulated earthquake motions for design purposes." *4th World Conference Eart. Engineering*

Santiago, pp. 145-160.

Kapur, J. and Kesavan, H. (1992). *Entropy optimization principles with applications*, Academic Press, San Diego, NY.

Kiureghian, A. Der (1981). "Structural Response to Stationary Excitation." *Journal of the Engineering Mechanics Division*, Vol. 106, No. 6, pp. 1195-1213.

Kiureghian, A. Der, and Neuenhofer, A. (1992). "Response spectrum method for multi-support seismic excitations." *Earthquake Engineering & Structural Dynamics*, Vol. 21, No. 8, pp. 713-740, DOI: 10.1002/eqe.4290210805.

Kramer, S. L. (1996). "Geotechnical earthquake engineering." *Prentice-Hall, Inc.*, Vol. 6, pp. 653, DOI: 10.1007/ 978-3-540-35783-4.

Kurtz, N. and Song, J. (2013). "Cross-entropy-based adaptive importance sampling using Gaussian mixture." *Structural Safety*, Vol. 42, pp. 35-44, DOI: 10.1016/j.strusafe.2013.01.006.

McKenna, F. (2010). Opensees User's Manual.

Mosalam, K. M., Alibrandi, U., Lee, H., and Armengou, J. (2018). "Performance-Based engineering and multi-criteria decision analysis for sustainable and resilient building design." *Structural Safety, Under Review*.

Novi Inverardi, P. L. and Tagliani, A. (2003). "Maximum entropy density estimation from fractional moments." *Communications in Statistics - Theory and Methods*, Vol. 32, No. 2, pp. 327-345, DOI: 10.1081/STA-120018189.

NTC08 (2008). Norme Tecniche per le Costruzioni, DM 14/01/2008.

Preumont, A. (1985). "The generation of non-separable artificial earthquake accelerograms for the design of nuclear power plants." *Nuclear Engineering and Design*, Vol. 88, No. 1, pp. 59-67, DOI: 10.1016/0029-5493(85)90045-7.

Priestley, M. B. (1965). "Evolutionary spectra and non-stationary processes." *Journal of the Royal Statistical Society. Series B (Methodological)*, Vol. 27, No. 2, pp. 204-237, DOI: 10.2307/2984191.

Rackwitz, R. (2001). "Reliability analysis-a review and some perspective." *Structural Safety*, Vol. 23, No. 4, pp. 365-395, DOI: 10.1016/S0167-4730(02)00009-7.

Rice, S. O. (1954). "Mathematical analysis of random noise." *Selected Papers on Noise and Stochastic Processes*, pp. 133-294, Dover Publicabions, New Mampshire.

Roberts, J. B. and Spanos, P. D. (1990). *Random Vibration and Statistical Linearization*, Wiley, Chichester.

Shinozuka, M. and Deodatis, G. (1988). "Stochastic process models for earthquake ground motion." *Probabilistic Engineering Mechanics*, Vol. 3, No. 3, pp. 114-123, DOI: 10.1016/0266-8920(88)90023-9.

Shinozuka, M. and Deodatis, G. (1991). "Simulation of stochastic processes by spectral representation." *Applied Mechanics Reviews*, Vol. 44, No. 4, pp. 191-204, DOI: 10.1115/1.3119501.

Spanos, P. D. and Solomos, G. P. (1983). "Markov approximation to transient vibration," *Journal of Engineering Mechanics*, Vol. 109, No. 4, pp. 1134-1150, DOI: 10.1061/(ASCE)0733-9399(1983)109:4(1134).

Talaat, M. and Mosalam, K. M. (2007). "Towards modeling progressive collapse in reinforced concrete buildings." *Structural Engineering Research Frontiers*, pp. 1-16, DOI: 10.1061/40944(249)14.

Talaat, M. and Mosalam, K. M. (2009). "Modeling progressive collapse in reinforced concrete buildings using direct element removal." *Earthquake Engineering and Structural Dynamics*, Vol. 38, No. 5, pp. 609-634, DOI: 10.1002/eqe.898.

Taufer, E., Bose, S., and Tagliani, A. (2009). "Optimal predictive densities and fractional moments." *Applied Stochastic Models in Business and Industry*, Vol. 25, pp. 57-71.

Vamvatsikos, D. and Allin Cornell, C. (2002). "Incremental dynamic analysis." *Earthquake Engineering and Structural Dynamics*, Vol. 31, No. 3, pp. 491-514, DOI: 10.1002/eqe.141.

Vanmarcke, E. and Gasparini, D. (1977). "Simulated earthquake ground motions." *4 International Conference on Structural Mechanics in Reactor Technology*.

Wang, Z. and Song, J. (2017). "Equivalent linearization method using Gaussian mixture (GM-ELM) for nonlinear random vibration analysis." *Structural Safety*, Vol. 64, pp. 9-19, DOI: 10.1016/j.strusafe.2016.08.005.

Xu, J. (2016). "A new method for reliability assessment of structural dynamic systems with random parameters." *Structural Safety*, Vol. 60, pp. 130-143, DOI: 10.1016/j.strusafe.2016.02.005.

Xu, J., Zhang, W., and Sun, R. (2016). "Efficient reliability assessment of structural dynamic systems with unequal weighted quasi-Monte Carlo Simulation." *Computers & Structures*, Vol. 175, pp. 37-51, DOI: 10.1016/j.compstruc.2016.06.005.

Yang, T. Y., Moehle, J., Stojadinovic, B., and Der Kiureghian, A. (2006). "An application of PEER performance-based earthquake engineering methodology," *8th U.S. National Conference on Earthquake Engineering*, No. 1448, pp. 1-10.

Zhang, X. and Pandey, M. D. (2013). "Structural reliability analysis based on the concepts of entropy, fractional moment and dimensional reduction method." *Structural Safety*, Vol. 43, pp. 28-40, DOI: 10.1016/j.strusafe.2013.03.001.